The Cryosphere, 19, 5299–5315, 2025
https://doi.org/10.5194/tc-19-5299-2025

The Cryosphere Open Access EGU

Formation of mega-scale glacial lineations far inland beneath the onset of the Northeast Greenland Ice Stream

Charlotte M. Carter[1,2], Steven Franke[3], Daniela Jansen[1], Chris R. Stokes[4], Veit Helm[1], John Paden[5], and Olaf Eisen[1,2]

[1]Alfred-Wegener-Institut Helmholtz-Zentrum für Polar- und Meeresforschung, Bremerhaven, Germany
[2]Faculty of Geosciences, Universität Bremen, Bremen, Germany
[3]Department of Geosciences, Tübingen University, Tübingen, Germany
[4]Department of Geography, Durham University, Durham, United Kingdom
[5]Center for Remote Sensing and Integrated Systems, University of Kansas, Lawrence, Kansas, United States of America

Correspondence: Charlotte M. Carter (charlotte.carter@awi.de)

Received: 11 April 2025 – Discussion started: 5 May 2025
Revised: 9 September 2025 – Accepted: 12 September 2025 – Published: 30 October 2025

Abstract. Rapidly-flowing ice streams drain the interior of the Greenland Ice Sheet, currently accounting for around half of its annual mass loss. The Northeast Greenland Ice Stream (NEGIS) is one of the largest, recognisable almost 600 km inland, and extends close to the central ice divide. Numerical ice sheet models are unable to accurately reproduce the configuration of the NEGIS, but understanding its bed properties and spatial and temporal evolution is critical to predicting its future contribution to sea-level change. Here, we use swath radar imaging to create a high-resolution Digital Elevation Model of the bed close to where the NEGIS initiates. Surprisingly, this reveals a landscape interpreted to include mega-scale glacial lineations (MSGLs) that are often assumed to be indicative of rapid ice stream flow (100s m yr^{-1}), under present-day flow velocities of only ~ 60 m yr^{-1}. Given that MSGLs are thought to form under much higher flow velocities, their presence so far inland at an onset zone raises important questions about their formation and preservation under ice streams, as well as past configurations of the NEGIS. Elongate bedrock landforms outside the current shear margins also suggest that the NEGIS was wider than its present configuration at some point in the past.

1 Introduction

The Greenland Ice Sheet (GrIS) is currently the largest contributor to global mean sea level rise from the polar ice sheets (Otosaka et al., 2023). Its mass loss has increased sixfold over the last 40 years (Mouginot et al., 2019), around 50 % of which is accounted for by dynamic discharge via ice streams (Shepherd et al., 2020). One of the most prominent is the Northeast Greenland Ice Stream (NEGIS), a 600 km long feature draining ~ 17 % of the GrIS (Krieger et al., 2019) via fast-flowing marine-terminating glaciers (Fig. 1a). The ice stream is characterised by several tributaries, the longest of which sharply narrows as it extends inland towards the central ice divide, and is also unusual in that there is no obvious topographic steering (Holschuh et al., 2019; Franke et al., 2020), meaning that the onset is not contained within a valley. The onsets of other ice streams in Greenland that are topographically unconstrained, such as Petermann Glacier (Chu et al., 2018), are often much wider and exhibit convergent flow into a main trunk, and lack such clearly defined shear margins, making the NEGIS unique in its geometry. Rather, the origins of the NEGIS have previously been attributed to subglacial water produced by exceptionally high geothermal heat fluxes in its onset zone (Fahnestock et al., 2001; Rysgaard et al., 2018; Smith-Johnsen et al., 2020), although this is disputed (Bons et al., 2021). Despite its importance, numerical ice sheet models are unable to fully replicate the NEGIS's unusual flow configuration (Aschwanden et al., 2016). This discrepancy between numerical ice sheet models and modern-day ice flow velocities is thought to be partly due to the missing parameter of ice crystallographic preferred orientation within the models (Gerber et al., 2023; Stoll et al., 2025), which can have an effect on the inferred basal drag

or friction coefficient (Rathmann and Lilien, 2022), but may also be related to the representation of basal conditions.

Whilst the modern flow configuration and surface velocity of the ice stream is well constrained by satellite observations (Joughin et al., 2018) (Fig. 1a), much less is known about the bed properties and the spatial and temporal evolution of the NEGIS, the understanding of which is crucial to elucidating the driving factors which influence the ice stream. Basal properties of the onset of the NEGIS have been constrained using single seismic lines, which were used to infer the, at least local, presence of saturated, high-porosity, deformable subglacial sediment (Fig. 1b) (Christianson et al., 2014; Riverman et al., 2019). The presence of a streamlined bed, with potential elongate subglacial landforms in the upper reaches of the NEGIS, has also been hinted at indirectly via off-nadir reflections from widely spaced radar lines (Franke et al., 2020). In terms of the evolution of the ice stream, a recent study has revealed that the shear margins and flow configuration in the onset zone of NEGIS were only established from around 2000 years ago (Jansen et al., 2024), questioning the assumption that the ice stream configuration had been stable throughout the Holocene (Fahnestock et al., 2001). Here, the amplitudes of folded internal reflection horizons from radio-echo sounding data indicate a record of the deformation of the ice stream, where the shear strain rates localised in narrow shear margins in the upstream part of the NEGIS $\sim$ 2000 years ago (Jansen et al., 2024). Indeed, evidence from internal stratigraphy has also shown rapid reconfigurations in ice flow trajectories and drainage basin areas in northeast Greenland over short (centennial) timescales during the Holocene (Franke et al., 2022a).

In order to further investigate the basal properties that lie beneath the onset of the NEGIS, this paper presents the first high resolution (25 m horizontal resolution, $\sim$ 10 m vertical resolution) Digital Elevation Model (DEM) of the subglacial topography, reconstructed from swath radar, which is capable of identifying individual subglacial bedforms. The DEM covers a $40 \times 60\,\mathrm{km}^2$ area surrounding the EastGRIP ice core site (Fig. 1b), where the ice thickness reaches 2.5 km and ice flow velocities are around $60\,\mathrm{m\,yr}^{-1}$. Previously, mapping of in situ subglacial bedforms under other active ice streams at such a high resolution has been achieved with conventional nadir-focused radar techniques, which derive bed elevation from closely-spaced radar lines and use interpolation (King et al., 2016; Bingham et al., 2017; Schlegel et al., 2022). These methods, whilst providing excellent observations, have an inherent limitation in their cross-track resolution and spatial coverage, in that direct point measurements of the bed are only possible in the along-track direction. Instead, with swath radar processing, there is no requirement to interpolate between these point measurements, as the direction of the arrival of energy in both the along-track and across-track directions can be estimated from the sequential acquisitions. Therefore, the topography can be reconstructed in high resolution over kilometre-wide strips, and the imaging of subglacial bedforms is possible at a lower logistical cost (Holschuh et al., 2020) and over a much wider spatial area.

Importantly, swath radar data surveys enable a view into the small-scale (10s to 100s of metres) subglacial topography and landforms that reside beneath active ice sheets. This has a range of advantages, from identifying geomorphological features, to enabling the incorporation of small-scale variations in basal topography within ice flow models, which can produce modelled ice motion patterns that diverge substantially from those utilising smoothly varying topography (Law et al., 2023). Two other similar surveys of swath radar data have been generated in Antarctica (Holschuh et al., 2020; Hoffman et al., 2023), which investigate the subglacial geomorphology beneath Thwaites Glacier and Hercules Dome. These data, alongside our DEM, provide crucial insight into the formation of subglacial landforms, which previously have generally only been accessible and studied within the context of deglaciated landscapes. For example, when elongate subglacial landforms are identified on a deglaciated landscape, they are utilised as a proxy to reconstruct previous ice sheet extent and dynamics (Margold et al., 2015a; Stokes et al., 2015). Mega-scale glacial lineations (MSGLs), for example, are generally associated with high flow velocities under ice streams (King et al., 2009; Stokes et al., 2013; Spagnolo et al., 2014). In addition, the elongation of these landforms has often been said to follow a down-flow morphological continuum, where they evolve from flow-perpendicular landforms at the onset (for example, ribbed moraines) to elongated flow-parallel MSGLs, as a product of increasing ice flow velocity and changing basal conditions, such as cumulative strain at the bed (Ely et al., 2016; Zoet et al., 2021; Vérité et al., 2021; Vérité et al., 2023). Similar transitions in evolution are also observed laterally, such as when crossing from the centre of an ice stream to its shear margin and beyond (Stokes and Clark, 2002a; Vérité et al., 2021). However, the inferred link between MSGLs, ice streaming, and the duration of their deformation related to cumulative strain at the base of the ice is largely qualitative with very few quantitative modelling studies (Jamieson et al., 2016; Ely et al., 2022; Vérité et al., 2024).

In addition, different formational mechanisms for MSGLs have been proposed and there is, as of yet, little consensus in the literature. Early ideas tended to focus on their construction via processes of subglacial deformation under high ice velocities (a velocity-duration product) (Clark, 1993). Others have proposed an erosional mechanism through the catastrophic discharge of turbulent subglacial meltwater (Shaw et al., 2008) or via the erosion of pre-existing sediments to reveal a streamlined surface of megaridges (Eyles et al., 2016). Indeed, some have focussed on the grooves between the ridges and suggested that MSGLs may be the erosional remnants or intervening ridges from a "groove-ploughing" mechanism, where roughness in the ice base passes over a bed of soft, saturated sediments (Clark et al., 2003). A more

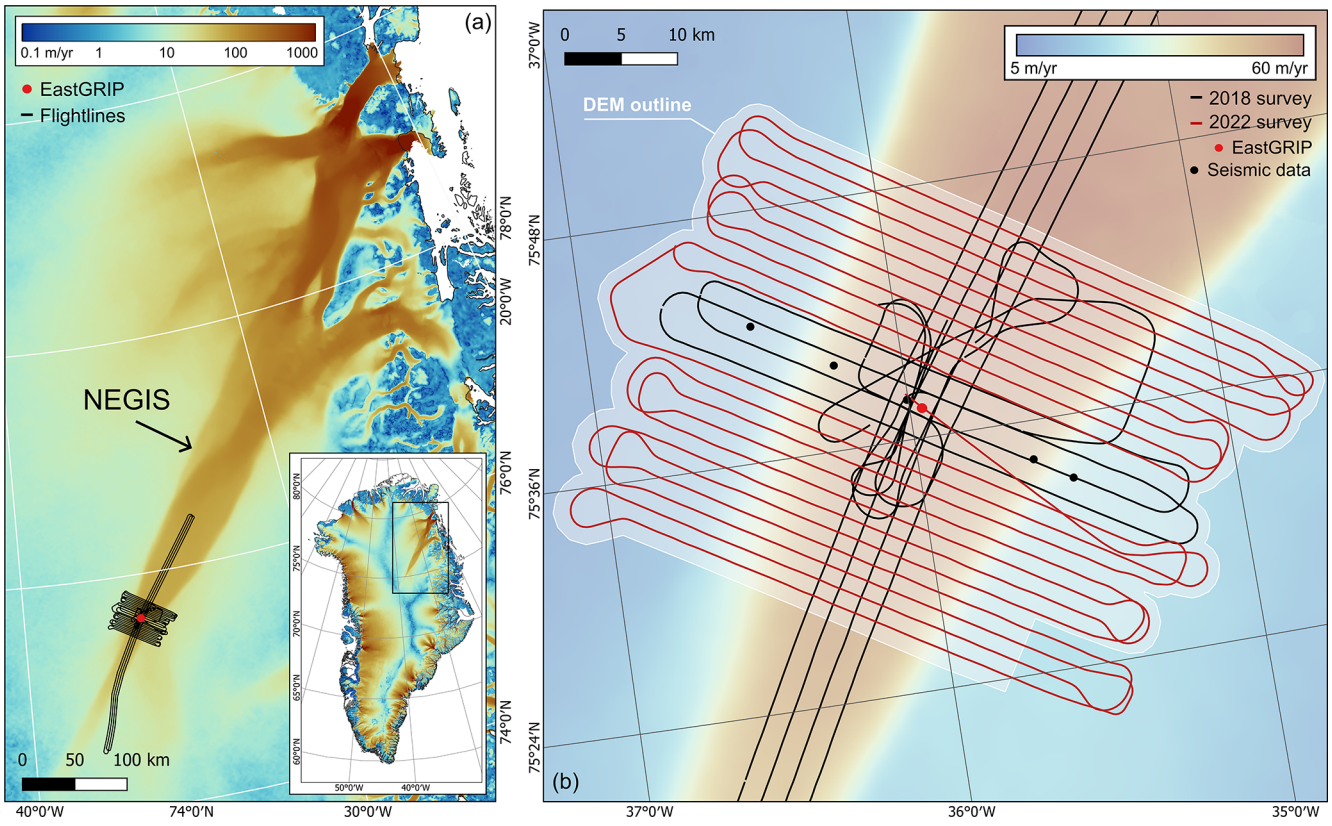

Figure 1. Overview of the study site in northeast Greenland. **(a)** NEGIS ice flow velocity (Gardner et al., 2022) with survey flightlines centred over the EastGRIP ice core site (red dot). Inset map shows ice flow velocity across Greenland on a logarithmic colour scale. **(b)** Survey flightlines in swath mode at the onset of NEGIS with an outline (light grey) of the generated DEM, and ice flow velocity in the background. Black dots show the locations of seismic data points from Christianson et al. (2014).

recent hypothesis invokes a rilling instability (Fowler, 2010), where the water flowing between ice and deformable subglacial sediment is unstable, and will form linear streams/rills separated by intervening ridges. Related to this hypothesis is the instability theory of the coupled flow of ice, water and till, which has successfully modelled the formation of a continuum of subglacial bedforms, including MSGLs (Ely et al., 2022). Although most work on MSGLs has utilised observations from the palaeo-record, geophysical data of their presence under extant ice sheets (e.g. King et al., 2009) offers a powerful tool to test some of these various formational hypotheses.

The data presented here comprise the first high-resolution subglacial topography survey beneath the onset of an ice stream in the deep interior of the GrIS, located around 600 km from the grounding line. The classification of the now visible geomorphological features provides insight into both the basal conditions of the ice stream and its spatial evolution. The identification of MSGLs beneath the onset also raises important questions around their formation and preservation beneath ice streams, given the relatively low ice flow velocities.

2 Methods

2.1 Generation of swath data

The Alfred Wegener Institute's ultra-wideband radar system (AWI-UWB) (Hale et al., 2016; Franke et al., 2022b) was used to map the cross-track topography at a horizontal resolution of 25 m, in swaths $\sim$ 2 km wide (Fig. 2). The majority of the flightlines were oriented perpendicular to the direction of ice flow, in order to reduce the possibility of artefacts that could be misinterpreted as flow-parallel subglacial landforms (Fig. 1b). Historically, the ability to resolve the detail of subglacial topography from airborne radar surveys has been dictated by along-track spacing, survey line spacing and along-track focusing, as conventional bistatic antenna airborne radar is unable to localise energy in the cross-track direction. Therefore, to produce a high-resolution digital elevation model of the bed, we apply swath processing techniques to ultra-wideband radar data collected by the AWI-UWB radar system in 2018 and 2022, surrounding the EastGRIP ice core site. Using a multi-element antenna array (Fig. 2a) means that information from sequential acquisitions, combined with phase differences in arrivals between

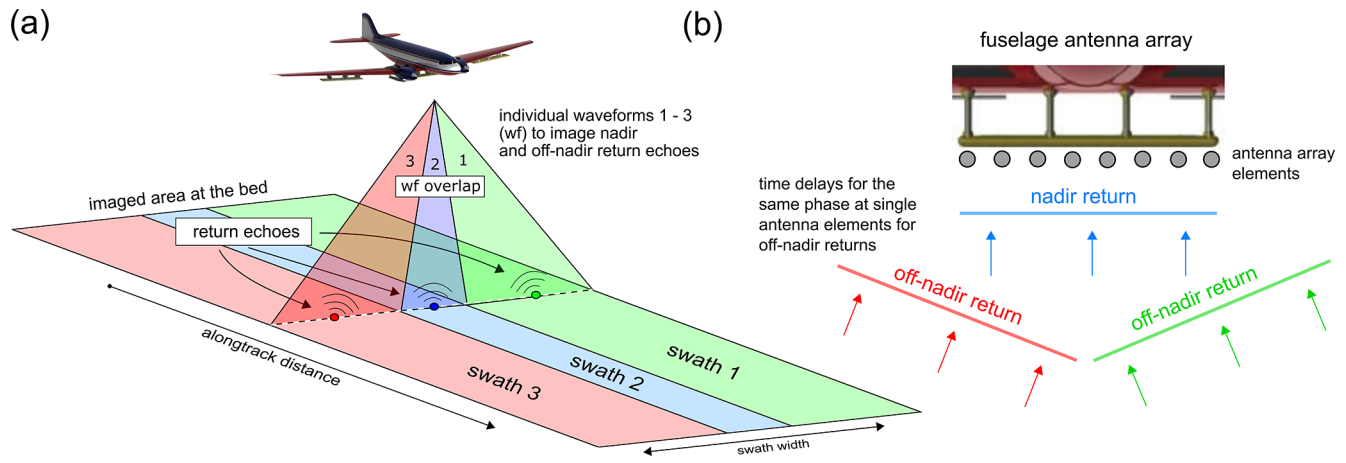

Figure 2. **(a)** Individual waveforms from a multi-antenna radar array used to image both nadir and off-nadir return echoes from the ice-bed interface. **(b)** Time delays for the same phase at single antenna elements are used to geolocate the off-nadir return echoes.

receiver elements (Jezek et al., 2011; Holschuh et al., 2020), can be used to estimate the direction of arrival for energy in both the along-track and across-track directions (Paden et al., 2010) (Fig. 2b). Application of the MUltiple Signal Classification (MUSIC) algorithm in the Open Polar Radar toolbox (Open Polar Radar, 2023) to SAR-processed radar data therefore allows mapping of the subglacial topography in three dimensions along a single flight line.

Along-track and fast-time averaging was applied to the SAR-processed data to improve the signal-to-noise ratio when tracking the bed return and cross-track surface. In the along-track direction, the depth range where the bed return was expected was selected using bed elevation values from BedMachine v.5 (Morlighem et al., 2017, 2022). The nadir bed return is picked in order to produce seed points from which the cross-track reflector is digitised, to geolocate off-nadir reflection information (Al-Ibadi et al., 2017). In the cross-track surface picking (Fig. 3a), the bed return power was fitted to a gaussian distribution in order to overcome the broad distribution and multiple peak bed returns from which the maximum is picked. Tracking of the bed pick is limited using a guided window based on a theoretical hyperbola of a flat bed, as there are often englacial reflections close to the bed return. A -2.5° static angle correction was also applied to account for tilting in the tracked cross-track surface, in order to align and overlap each swath accurately. For each trace, after cross-track surface tracking, the hyperbola of the bed return is range migrated, including the refraction of air to ice, to convert the surface tracking to depth (Fig. 3b). Here, upwarping at the edges of each swath introduced some artefacts into the data, as spreading of the bed return energy reduced the accuracy of the surface tracking. Whilst this could have been excluded from the final DEM, reducing the swath width prevented overlap of each swath, meaning that landforms could not be mapped distinctly. The range migrated data produced a point cloud, which is projected from the reference frame to geographic coordinates (latitude and longitude) using the true heading and flight trajectory from the radar data. The final DEM raster is then interpolated from the georeferenced point cloud dataset using inverse distance weighting, at a pixel spacing resolution of 25 m and a vertical resolution of ~ 10 m. The resulting product is a three-dimensional tomographic image of the ice base, with swath widths of ~ 2 km.

2.2 Characterisation of the subglacial landscape

In order to characterise the subglacial landscape, digital geomorphological mapping of the landforms was carried out in QGIS v3.26.3 (QGIS, 2025) (Fig. 4). Multiple hillshade directions and contour lines were utilised to define the edges of landforms (Chandler et al., 2018), which were manually delineated across the DEM. The landforms were initially categorised, without interpretational bias, as geomorphic ridges, lineations, channels, and basins. Lineations (Fig. 4a) were identified as linear, low relief, and flow-parallel features. Geomorphic ridges, in contrast to lineations, are landforms that are less consistent in their width and less elongate, meaning that they were more circular or irregularly shaped. Channels are incised valleys that cut across the landscape as linear to sinuous depressions (Fig. 4e). Basins were mapped as flatter areas in topographic low points (Fig. 4d), often between larger ridges, with a much smoother appearance compared to the areas of geomorphic ridges.

Elongation ratios were calculated in QGIS as the length of a minimum bounding rectangle divided by the width. As the swath processing introduced some artefacts into the DEM, due to upwarping at the edge of each swath creating flow-perpendicular rises in elevation, only landforms which are clearly identifiable as geomorphological features, and could definitively be observed crossing multiple swath widths, were mapped.

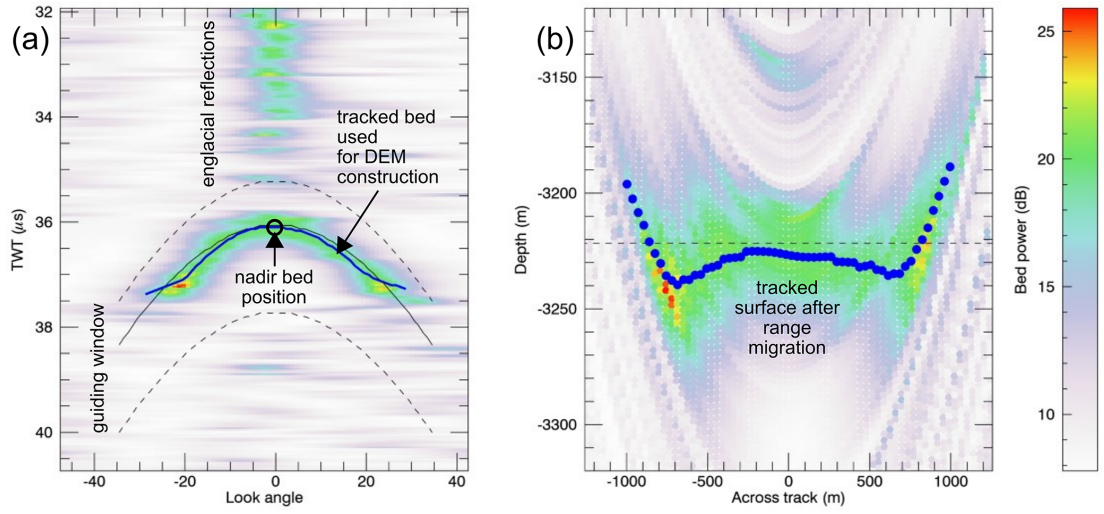

Figure 3. **(a)** Cross-track surface tracking at each nadir bed position produced from the MUSIC algorithm (Paden et al., 2010). **(b)** The tracked surface is range migrated to convert the two-way travel time values to depth.

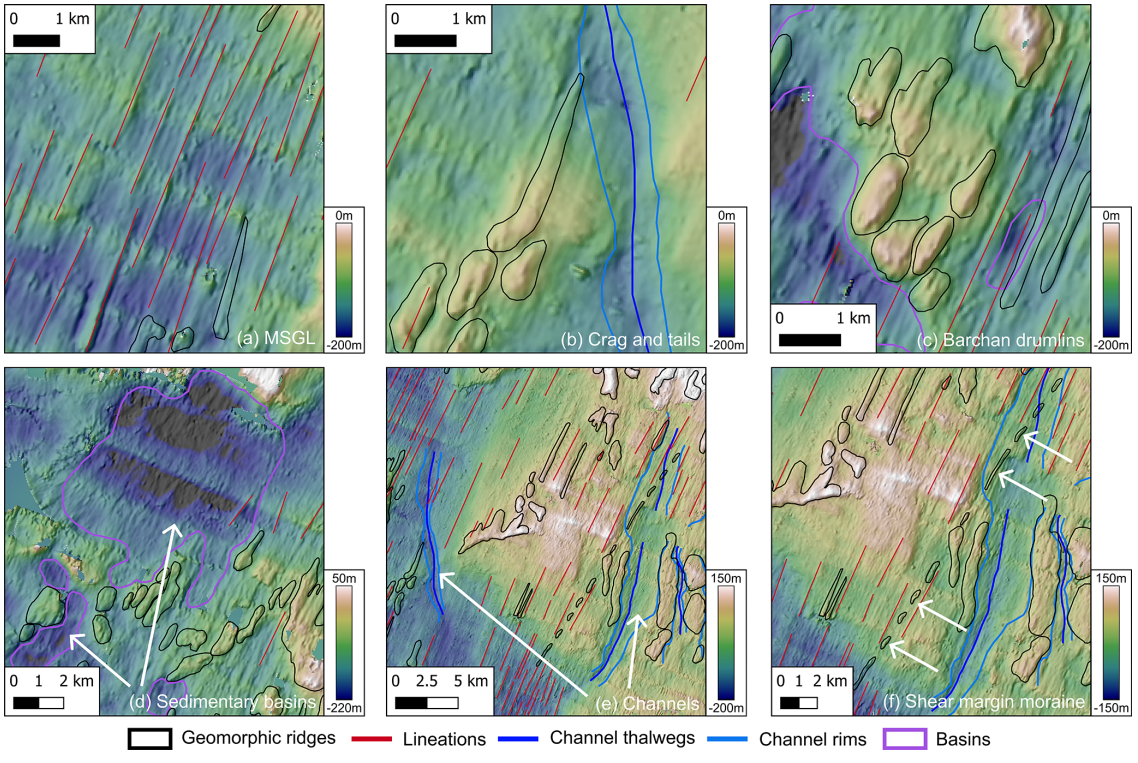

Figure 4. Examples of subglacial landforms identified beneath the onset of the NEGIS. The initial non-interpretational mapping of lineations (red lines), geomorphic ridges (black outlines), channels (dark blue thalwegs, light blue rims) and basins (purple outlines) is shown in each panel. These landforms were then interpreted as described below, examples of which are shown in each panel: **(a)** Mega-scale glacial lineations. **(b)** Crag and tails. **(c)** Barchan/erosional drumlins. **(d)** Sedimentary basins. **(e)** Meltwater channels. **(f)** Shear margin moraine.

2.3 Comparison of landforms to velocity data and shear margins

The NASA MEaSURES ITS_LIVE velocity mosaic (Gardner et al., 2022) was used to derive the streamlines of the current velocity field, as well as the overlying surface velocity related to each landform. The mean velocity value within each polygon was used as a representative value for each individual landform. The shear margins of the ice stream were delineated where the shear strain rate was at its maximum

value from multiple cross-profiles. The shear strain rate was derived from TerraSAR-X ice velocity data (Hvidberg et al., 2020). Relative locations of subglacial landforms within or outside of the shear margins were determined using the outermost shear margin where the shear margins overlap, and the polygon delineating the landform had to be contained entirely within the shear margin boundaries.

3 Results

High resolution subglacial geomorphology at the onset of the NEGIS

A detailed image of the subglacial landscape is shown in Fig. 5, with our mapping of the landform assemblage shown in Fig. 6a (see also Fig. 4). Low relief, highly elongated lineations are interpreted as MSGLs (Fig. 4a) and are almost entirely constrained within the modern shear margins of the NEGIS (Fig. 5). The elongation ratios of these lineations range between 7.7 : 1 and 59.2 : 1, with the more elongate features generally located beneath the central trunk of the NEGIS (Fig. 6b). MGSLs can be identified as linear, low relief, and flow-parallel features, which generally have elongation ratios greater than 10 : 1, and are generally consistent in terms of width (Stokes and Clark, 2002b; Stokes et al., 2013; Ely et al., 2016). The majority are oriented in the direction of the overlying surface flow, although some close to the shear margins are oriented at an angle up to 13° away from the trajectory of the current flow field. Heights of the MSGLs have a mean value of 66.5 m, and range between 21 m (minimum) and 148.4 m (maximum). The MSGLs range from 968 to 7397 m in length, with a mean value of 3025 m (Fig. 6c), but some are truncated by ridges that have a rougher appearance in the landscape. In addition, there are instances where the ridges appear to act as seed-points for the MSGLs, which then continue downstream into the sedimentary basins and have a much smoother appearance (see identified MSGLs in Fig. 5).

Geomorphic ridges were subsequently interpreted as three different categories: crag-and-tails (Fig. 4b), barchan drumlins (Fig. 4c), or a shear margin moraine (Fig. 4f). They are mostly interpreted as bedrock features, resembling crag and tails (Fig. 4b, metrics in Table A1). These are elongate features with a steep stoss side on a bedrock crag and lee side tails oriented in the direction of overlying ice flow. They are differentiated from MSGLs by their higher relief and with stoss-side crags having a rougher appearance, with a smoother tapering lee-side tail that is usually composed of unconsolidated sediment (Dowdeswell et al., 2016; Nitsche et al., 2016). There are some potential barchan, or erosional, drumlins (sensu Eyles et al., 2016), which are identified based on the grooves carved into the bedrock ridges, bisecting a larger "parent" drumlin into smaller outcrops that are grouped together in a crescentic shape (Fig. 4c). The bedrock ridges are clustered in groups, particularly in the southwest of the survey area, and are present both within and outside of modern shear margins, more evidently on the western side. The distribution of elongation ratios of these ridges demonstrates that they show some degree of elongation outside of the shear margins, as well as inside (Fig. 6d). However, in the absence of seismic data directly overlying these areas of hypothesised bedrock, this interpretation may have a higher level of uncertainty. Some geomorphic ridges (e.g. in the centre of Fig. 4e), with a long axis 45° oblique to the MSGLs and shear margins, may represent deformed ribbed bedforms, which are a transitional bedform resulting from the deformation of flow-transverse ridges (Vérité et al., 2023, 2024).

A long, low relief, narrow feature aligned closely with the south-eastern shear margin, but clearly misaligned with ice flow direction (see yellow arrows in Fig. 5), is interpreted as a lateral shear margin moraine (Stokes and Clark, 2002a). This is based on its proximity and alignment with the shear margin, its continuity across multiple swaths, and its relief of between 30 to 40 m that is prominent in the surrounding landscape (Fig. 4f). The ridge appears to be dissected in places, but this is likely due to artefacts at the edge of each overlapping swath (see Methods and Fig. 3a). This dissection may be a function of the ridge's orientation, which is oblique to the flightlines, as mapped MSGLs are less subject to this effect and appear continuous across multiple swaths. Riverman et al. (2019) also identified a shear margin moraine with similar dimensions of ~ 500 m width and ~ 50 m height, and orientation nearly parallel to ice flow, although it is not clear if we image exactly the same bedform.

Other features include depressions within which are likely to be softer/unconsolidated sediments, rather than hard bedrock, as might be suggested by their smoother appearance (Roberts et al., 2019; Dowdeswell et al., 2016). Previous seismic surveys crossing the topographic low point beneath the north-western shear margin demonstrate acoustic impedance values that correspond to soft, deformable till, indicating the presence of saturated subglacial sediment in this region, including where the MSGLs are identified (Christianson et al., 2014; Riverman et al., 2019). These sediments contained within the basins (Fig. 4d) appear as flatter areas in topographic lows, which are often downstream of bedrock features, the largest of which has an area of 49 km^2. Some large (between 0.5–3 km wide) incised channels with undulating thalwegs are also identified, often deviating around topographic highs and cutting across the landscape both inside and outside of the ice stream (Fig. 4e). These are interpreted as large meltwater channels, and potentially tunnel valleys which indicates incision by subglacial meltwater (Livingstone and Clark, 2016; Kehew et al., 2012), although the possibility remains that they are part of a preserved fluvial network.

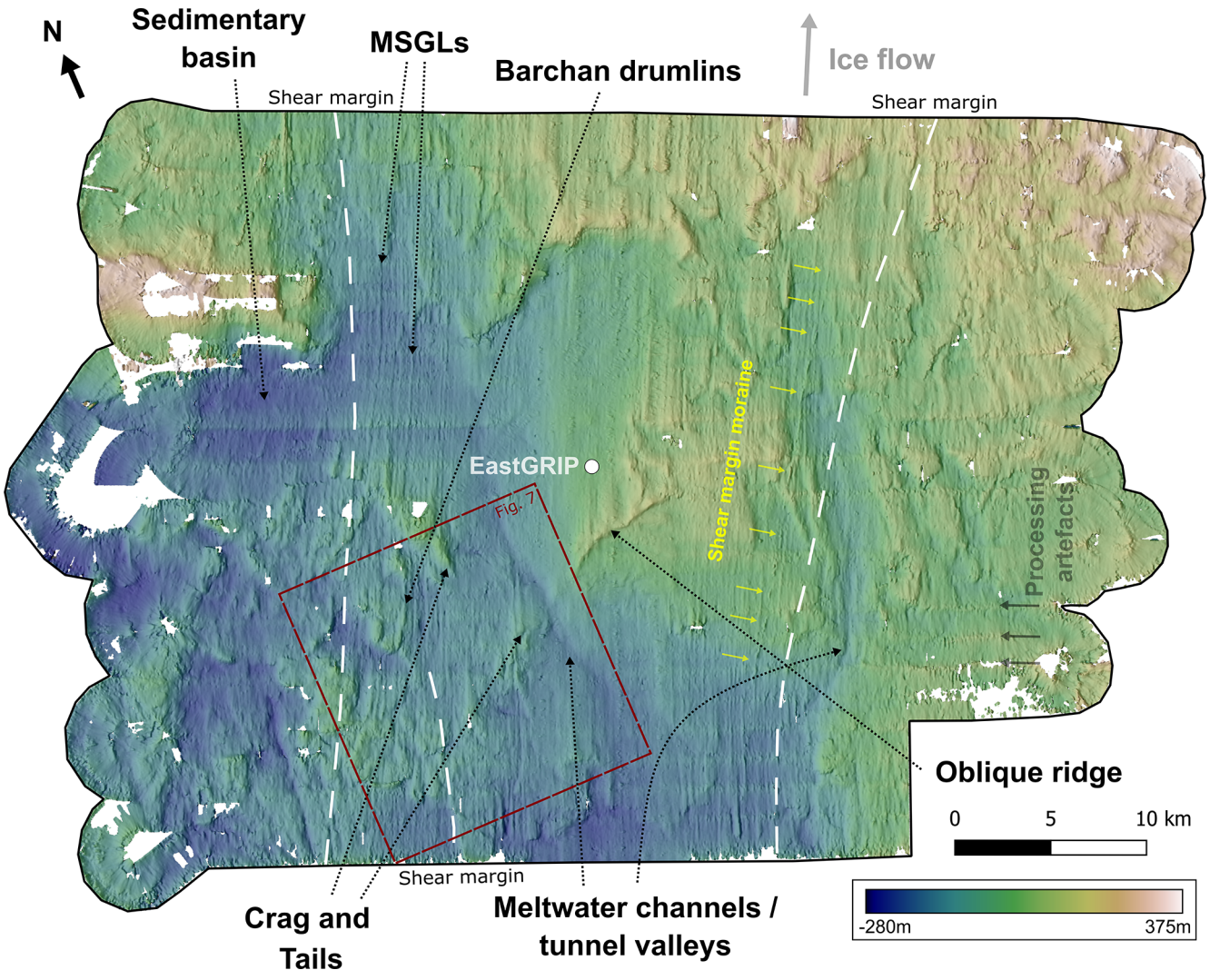

Figure 5. Subglacial topography produced from swath radar measurements at the onset of NEGIS (Carter et al., 2025). The hill-shaded DEM (referenced to WGS84) allows interpretation of an assemblage of subglacial landforms, characteristic of ice streaming, such as mega-scale glacial lineations, crag and tails, and barchan drumlins. Location of the survey shown in Fig. 1 and the red box shows the location of Fig. 7. Arrows on top indicate True North and direction of ice flow. The line delineating the location of the shear margin (maximum shear strain rate) is dashed, as this represents the central point of the broader transition between slow and fast flow (the shear zone).

4 Discussion

4.1 Implications for the basal conditions and spatial evolution of the NEGIS

Classification of the geomorphology beneath the onset of the NEGIS allows us to infer some aspects of the basal properties, as the differing regions of subglacial landforms would suggest heterogeneity of the bed. The geomorphology bears close resemblance to a "mixed bed" landform assemblage (Fig. 7), composed of a combination of hard bedrock outcrops interspersed with softer sediments and subglacial bedforms, such as those identified on palaeo-ice stream beds in west Greenland (Dowdeswell et al., 2014), the Amundsen Sea Embayment (Graham et al., 2009), western Northern America as part of the Late Wisconsin Cordilleran Ice Sheet (Eyles et al., 2018), and the North Sea (Roberts et al., 2019) (Fig. 7). These types of subglacial landscapes are characterised by the combined presence of crag and tails, drumlins, and highly elongate lineations, and thought to be formed under ice streams (Graham et al., 2009; Dowdeswell et al., 2014; Roberts et al., 2019; Eyles et al., 2018). Previous seismic data from around the EastGRIP ice core site (Christianson et al., 2014) showed saturated, high-porosity, presumably deforming sediment within the main trunk of the ice stream, and non-deforming and more compacted sediments outside of the main trunk. However, the presence of crag-and-tails would imply additional bedrock outcrops in the broader re-

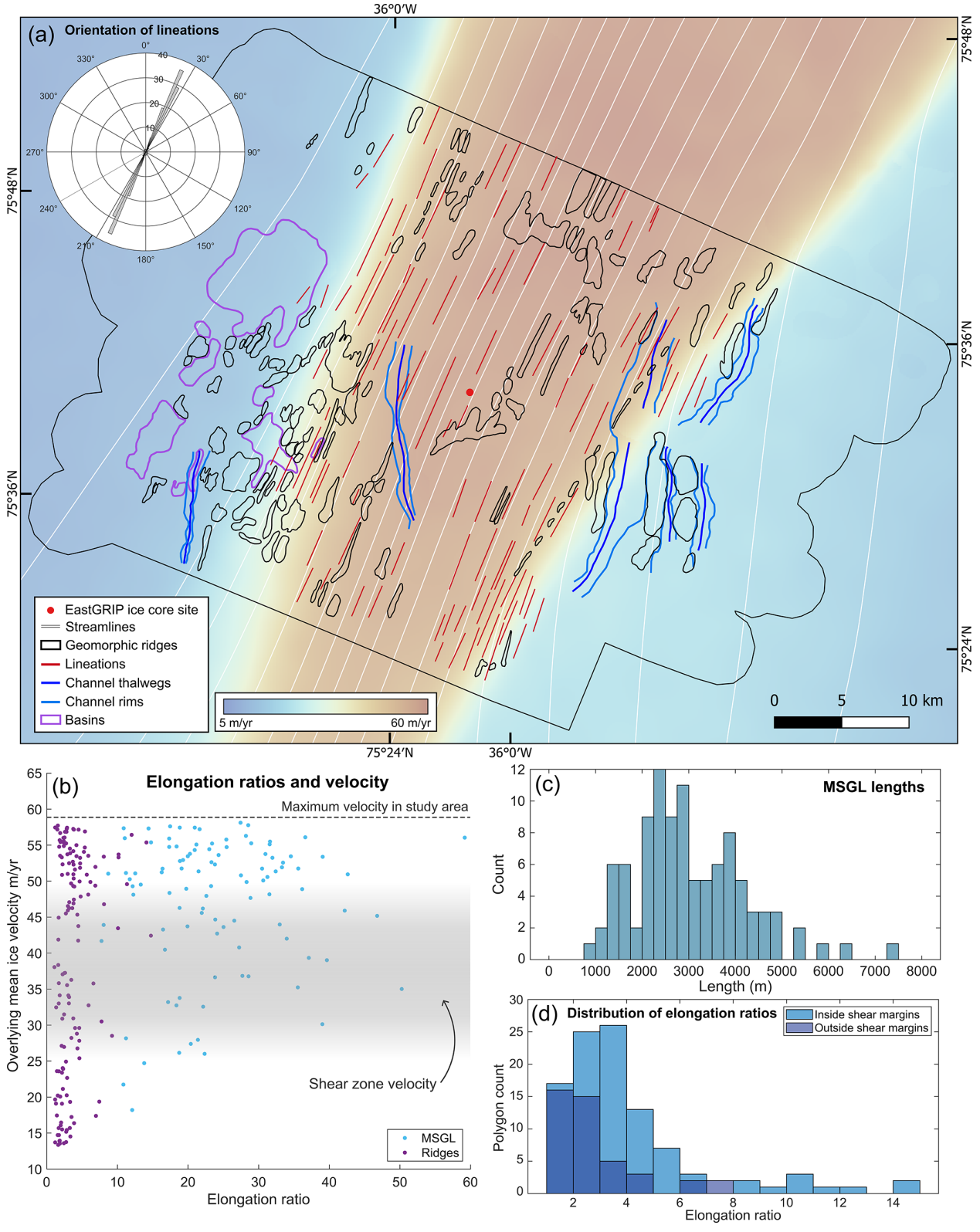

Figure 6. Subglacial landform mapping related to the overlying ice dynamics. **(a)** Geomorphological mapping of the subglacial topography, with surface ice flow velocity (Gardner et al., 2022) and streamlines (Hvidberg et al., 2020), which are flow-parallel lines, illustrating the direction of flow of the current steady-state velocity field. Inset polar histogram shows the orientation distribution of the MSGLs. **(b)** Scatter plot showing the elongation ratios of the MSGLs and geomorphic ridges compared to surface flow velocity. **(c)** Histogram of MSGL length. **(d)** Histogram of the elongation ratios of the geomorphic ridges, both within and outside of the modern shear margins of the NEGIS.

gion of the onset now visualised by our new DEM. Christianson et al. (2014) infer from their observations that an underlying layer of dilatant till might explain the presence of the ice stream in this location and its lack of a major subglacial trough, but our observations of a mixed bed landform assemblage would suggest that the characteristics of the bed are perhaps more heterogenous than previously recognised.

Within this mixed-bed assemblage, the distribution of the identified subglacial landforms can be used to infer changes in the location of the ice stream shear margins, using the crag-and-tails, which are commonly used as indicators of fast palaeo-ice flow (Dowdeswell et al., 2010; Nitsche et al., 2016; Dowdeswell et al., 2016). The degree of elongation of crag-and-tails outside the present shear margin is similar to those inside of the shear margins (Fig. 6c, Table A1), indicating a potential spatial evolution of the shear margins of the NEGIS. It suggests that they could have been subject to similar flow conditions as inside the shear margins of the current ice stream at some point in the past, as the current overlying ice velocity conditions outside of the shear margins are slower, and not streaming (10 to 25 m yr^{-1}, Fig. 6b). The crag-and-tails are more prevalent on the north-western side of the ice stream compared to the southeast, which correlates with internal folding of ice horizons that demonstrate a "jump" between an active and inactive section of the north-western shear margin, where the margin has shifted inwards (Jansen et al., 2024). The south-eastern shear margin, however, has a much more abrupt transition between the slow-flowing and fast-flowing ice inside of the ice stream trunk. The transitory nature of the north-western shear margin could, therefore, be related to a potential narrowing of the ice stream associated with the localisation of the shear margins, as streaming conditions would have overlain the ridges currently outside of the shear margins. Therefore, we propose that the ice stream may have been up to 10 km wider at some point in the past, or experienced convergent or a slightly different direction of flow prior to the localisation of the current shear margins (Bons et al., 2016; Jansen et al., 2024). The relative lack of crag-and-tails, as well as the preservation of a potential shear margin moraine evident along the south-eastern shear margin, suggest a more stable configuration on this side.

4.2 Implications for MSGL formation

Subglacial landforms used to reconstruct palaeo-ice streams, such as drumlins and MSGLs, have often been argued to represent a subglacial morphological continuum that evolves with cumulative basal slip speed (Stokes et al., 2013; Ely et al., 2016; Barchyn et al., 2016; Zoet et al., 2021; Ely et al., 2022; Vérité et al., 2024). Along this continuum, ice flowing at velocities of 10s to < 100 m yr^{-1}, i.e. similar to the velocity at the onset of NEGIS, has been associated with landforms oriented perpendicular to ice flow direction known as ribbed moraines, but merging into classic drumlins as velocity increases (Stokes et al., 2013). Hence, ice stream onset zones are generally thought to be associated with landforms that are transverse to ice flow, or oriented in the direction of ice flow but with low elongation ratios that are more characteristic of drumlins, rather than MSGLs (King et al., 2007; Anderson and Fretwell, 2008; De Angelis and Kleman, 2008). When modelled, as ice velocities increase to 100s m yr^{-1}, drumlins have been hypothesised to evolve and elongate into MSGLs (Stokes et al., 2013; Barchyn et al., 2016; Ely et al., 2022; Vérité et al., 2024), but there is little work that quantitatively links bedform elongation to ice flow/slip speed and the assumptions are mostly qualitative.

The geomorphological signature beneath the onset of NEGIS has a clear ice streaming imprint with the presence of MSGLs, which is perhaps surprising given that ice velocities within the study area currently peak at 58 m yr^{-1}. All previous observations of MSGLs beneath active ice streams are associated with ice velocities > 100 m yr^{-1}, such as the landforms detected beneath the main trunks of Rutford Ice Stream (Schlegel et al., 2022) (380 m yr^{-1}) and Thwaites Glacier (Holschuh et al., 2020) (between 100 and 400 m yr^{-1}), which have formed under continuous and relatively stable high-velocity ice streaming conditions (Woodward and King, 2009; Alley et al., 2021; Gudmundsson and Jenkins, 2017). The setting of these ice streams contrast with the temporally and spatially variable NEGIS (Franke et al., 2022a), with its slower (< 60 m yr^{-1}) velocities at the onset. To our knowledge, the only other high-resolution DEM of a modern ice stream onset zone (King et al., 2007) revealed classic drumlin forms (elongation ratios 1 : 1.5 to 1 : 4) and a potential ribbed moraine under Rutford Ice Stream, West Antarctica, where velocities accelerate from 72 to > 200 m yr^{-1}. The landforms beneath the onset zone of the Rutford Ice Stream are much less elongate, but are forming beneath higher ice flow velocities than our study area of the NEGIS. Furthermore, the location of the MSGLs in our study, 600 km from the grounding line and only ~ 200 km from the main ice divide, is also the furthest inland that MSGLs have been identified beneath a modern ice sheet. Even so, ice stream onset zones clearly can extend very close to ice divides in both palaeo (Margold et al., 2015a, b) and modern settings (Bamber et al., 2000). Indeed, there are numerous examples from the palaeo-record that show ice stream imprints extending very close to the inferred position of ice divides (Hodder et al., 2016; Rice et al., 2020; Dubé-Loubert et al., 2021; Rice et al., 2024). However, it is very rare for MSGLs to be identified/mapped so close to an ice divide.

There are a number of hypotheses that might explain the presence of MSGLs beneath the modern-day slow ice velocities observed at the onset of the NEGIS. Firstly, one possibility is that the MSGLs are akin to bedrock mega-grooves and, therefore, their length is not directly related to ice velocity (Newton et al., 2018). However, we reject this hypothesis, as the morphometric characteristics of the MSGLs here are different to those relating to bedrock mega-grooves (New-

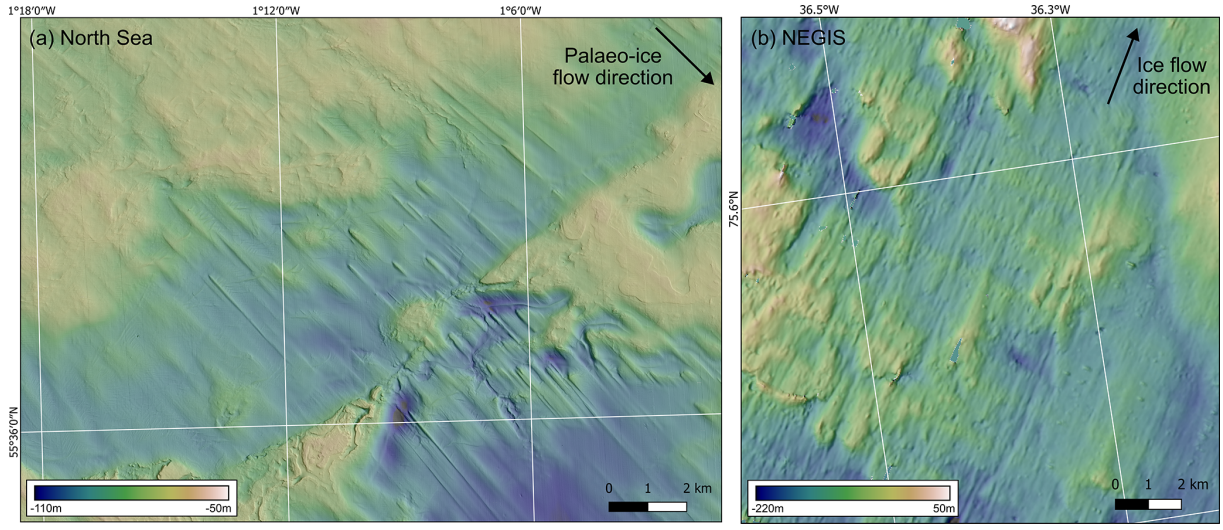

Figure 7. Comparison of mixed-bed landform assemblages. **(a)** North Sea bathymetry data showing streamlined bedforms and bedrock highs (Roberts et al., 2019). **(b)** Bedrock features beneath the onset of NEGIS (inset in Fig. 5).

ton et al., 2023). The heights of the MSGLs average 66.5 m, which are much greater than the depths seen in bedrock mega-grooves (5–15 m; Newton et al., 2023). Whilst some studies have shown the majority of amplitudes of MSGLs to have low heights (between 0.4–38.1 m; Vérité et al., 2024), MSGLs of the scale identified here have also been observed beneath Thwaites Glacier, where elongated bedforms composed of soft till locally exceed 100 m in height (Alley et al., 2021), as well as in past ice streams off the Antarctic Peninsula (Canals et al., 2000). The contrast of the rougher bedrock outcrops to the smoother appearance of the MSGLs would also indicate that this is a mixed bed assemblage (Roberts et al., 2019), as the landscape is akin to a transitional "mixed bed" zone, where streamlined bedrock features and MSGL occur adjacently as the subglacial bed changes between hard and soft material (Eyles and Doughty, 2016; Mulligan et al., 2019).

In addition, the role of subglacial meltwater and its potential contribution to MSGL formation in this context is difficult to constrain. Subglacial hydropotential modelling has indicated that water is concentrated into and along the shear margins (Christianson et al., 2014; Franke et al., 2021), and moves through this region in a distributed system with only limited regions of continuous channelisation (Riverman et al., 2019), suggesting that it has a limited role in bedform development. Observations from phase-sensitive radar measurements at the EastGRIP ice core site quantify basal melt rates at $0.19 \pm 0.04\,\mathrm{m\,a^{-1}}$ (Zeising and Humbert, 2021), which is suggested to arise from the subglacial meltwater system, but information on subglacial water volume is very limited. Subglacial drainage cascades have also been observed, albeit much further downstream, by differential satellite synthetic aperture radar interferometry (DInSAR) (Andersen et al., 2023). As the amount of subglacial water cumulatively increases downstream, smaller amounts of subglacial water are likely to exist at the onset further upstream, but below the detection limit of DInSAR.

Secondly, it could be argued that a plausible hypothesis to explain the presence of the MSGLs under this part of the NEGIS, is that the study area experienced higher ice velocities in the past, after which the MSGLs have simply been preserved. This might therefore suggest that ice velocities under this part of the NEGIS were much higher ($> 100\,\mathrm{m\,yr^{-1}}$) at some point in the past. However, it is unlikely that the NEGIS experienced higher ice velocities prior to the localisation of the shear margins 2000 years ago (Jansen et al., 2024). The folds in the isochrones observed at the NEGIS onset by Jansen et al. (2024) are consistent with folding due to convergent ice flow (e.g. similar to Petermann Glacier), which are then sheared where they are intersected by the shear margins, causing them to rotate and tighten. The timing of this intersection of the folds by the shear margin is constrained to 2 ka by both the offset of $\sim$ 55–75 km of the fold hinges (as they are advected with ice flow over $\sim$ 2000 years) as well as the cessation of fold amplification at 2 ka. When the shear margins localised in their current location, the ice stream was decoupled from the interior of the ice sheet, as the rotation of the orientation of the ice crystal basal planes lead to mechanical weakening in the shear margins (Gerber et al., 2023), which in turn facilitates localised deformation and the faster flow observed at present. Higher velocities would have produced higher shear strain within the margins, for which the analysis of the fold amplitudes by Jansen et al. (2024) did not show any evidence. Modelling of the ice stream dynamics of the northeastern sector of the Greenland Ice Sheet since the Last Glacial Maximum has also shown no evidence of higher velocities within the interior of the ice sheet, prior to the formation of the NEGIS (Tabone et al., 2024). Thus, we would

consider the plausibility of these MSGLs being formed from a faster configuration of the NEGIS to be unlikely.

Thirdly, it could be argued that the MSGLs under the onset of the NEGIS were formed by the current slow ice velocities over much longer (multi-millennial) timescales (Clark, 1993), where the present NEGIS has been very stable in this location at this flow speed. However, it has been shown that the NEGIS is a relatively young ice stream (< 2000 years) and that this sector of Greenland has undergone drainage basin reconfiguration over the Holocene (Franke et al., 2022a; Jansen et al., 2024). Earlier configurations of now-extinct ice streaming in the northeastern part of the ice sheet during the Holocene did not reach so far into the interior (Franke et al., 2022a; Tabone et al., 2024), instead draining a more northerly part of the ice sheet, indicating that the NEGIS as seen today is a relatively recent feature established within the last 2000 years (Jansen et al., 2024). Thus, although we are unable to rule out that the MSGLs may have formed by slow flow over a much longer duration (> 2000 years), we view this as unlikely because they correspond to the margins of the present enhanced flow, rather than everywhere across the study area. Indeed, if that were the case more generally, then MSGLs would be far more common on both palaeo and modern ice sheet beds. As well, there is evidence from the palaeo-record that ice streams can switch on and off over just a few hundreds of years. During deglaciation of the Laurentide Ice Sheet, it has been shown that around 40 % of ice streams operated for < 2000 years (Stokes et al., 2016; Margold et al., 2018), although very few of these ice streams record MSGLs so close to the inferred ice divide.

Whilst we cannot rule out an episode of enhanced flow at this location in a previous glaciation, the sedimentary basins outside of the northwestern shear margin (Fig. 6) show little evidence of MSGL formation, similar to our observations within the shear margins. This would mean that the ice stream would have formed in the same configuration as observed today, potentially with a higher velocity, to produce the observed MSGLs. Even so, if this had occurred, this would then suggest that MSGLs can be preserved for 100s to 1000s of years under relatively slow ice velocities. Rather, we propose that these MSGLs within the current shear margins, are likely to have formed in situ under modern-day slow ice velocities ($< 60\,\mathrm{m\,yr^{-1}}$), over the 2000 years in which the NEGIS onset has existed at this location, questioning the paradigm that they are exclusively associated with fast ice flow. This potentially could be attributed to the presence of highly deformable sediments, which have high porosity and high dilatancy (Christianson et al., 2014; Riverman et al., 2019), where these MSGLs have been identified.

5 Conclusions

In conclusion, high-resolution bed topography data from swath radar enables key observations into the basal conditions of an ice stream, as well as its potential spatial evolution. The identification of the previously unseen subglacial geomorphology beneath the onset of the NEGIS allows insight into the processes under which these landforms form. The presence of MSGLs so far inland under the NEGIS is a surprising discovery, given that ice velocities are $< 60\,\mathrm{m\,yr^{-1}}$ and the study area is only ~ 200 km from the ice divide. We deem it unlikely that the MSGLs were formed by slow ice flow over a much longer duration than 2000 years, but are unable to rule out the possibility that a previous episode of fast flow created the MSGLs, which would have since been preserved under ice flow conditions similar to present. However, we view this as unlikely given that the folding of the internal stratigraphy and shear strain rates of the margins indicate a slower, confluent flow regime preceding the formation of the shear margins. Rather, our favoured interpretation is that the MSGLs are the product of the relatively low ice velocities ($10\mathrm{s\,m\,yr^{-1}}$) observed today, within the 2000-year timescale of the current configuration of the NEGIS. If correct, these observations may prompt a re-evaluation of some models of MSGL formation and their use as an indicator of high ($> 100\mathrm{s\,m\,yr^{-1}}$) ice velocities, but further work, such as a multitemporal analysis, is required to examine whether the features are relicts from a previous flow regime or are actively forming under current conditions.

Appendix A

Table A1. Quantitative metrics of geomorphic ridges mapped.

		Geomorphic ridges	Geomorphic ridges (within shear margins)	Geomorphic ridges (outside of shear margins)
Sample size		144	101	43
Length	Min	409.5	558.3	409.5
	Max	7593.7	5860.1	7593.7
	Mean	2009.3	2004.2	2021.2
	Median	1680.9	1705.7	1533.3
	SD	1230.3	1108.9	1491.8
Width	Min	203.5	203.5	223.6
	Max	3680.2	3680.2	2105.6
	Mean	663.2	619.8	764.9
	Median	562.8	505.6	708.6
	SD	501.9	518.2	450.8
Elongation ratio	Min	1.1	1.1	1.2
	Max	14.7	14.7	7.7
	Mean	3.7	4.1	2.8
	Median	3.0	3.4	2.3
	SD	2.5	2.7	1.7
Height	Min	27.0	28.0	27.0
	Max	212.3	212.3	199.2
	Mean	80.1	75.9	90.5
	Median	72.5	68.6	80.6
	SD	37.1	35.0	40.2

Data availability. The DEM raster GeoTiff constructed from AWI UWB swath mode RES data is available at PANGAEA (https://doi.org/10.1594/PANGAEA.972422, Carter et al., 2025). AWIs airborne radar data is publicly accessible through the Radar Data over Polar Ice Sheets viewer hosted by the Marine Data Portal (https://marine-data.de/viewers, last access 20 October 2025) and available for download at PANGAEA. Multibeam echosounder bathymetric data from the North Sea (Fig. 7) was downloaded from the UK Hydrographic Office under the Civil Hydrography Programme (https://data.admiralty.co.uk/portal/apps/sites/#/marine-data-portal, last access: 20 October 2025).

Author contributions. OE, SF, and CMC conceptualised the study. DJ and JP collected the survey data, which was processed by VH, SF, and CMC, with the method being developed by VH. CMC prepared the manuscript with contributions from all co-authors.

Competing interests. The contact author has declared that none of the authors has any competing interests.

Disclaimer. Publisher's note: Copernicus Publications remains neutral with regard to jurisdictional claims made in the text, published maps, institutional affiliations, or any other geographical representation in this paper. While Copernicus Publications makes every effort to include appropriate place names, the final responsibility lies with the authors. Also, please note that this paper has not received English language copy-editing. Views expressed in the text are those of the authors and do not necessarily reflect the views of the publisher.

Acknowledgements. We would like to thank David Roberts, David Evans, Johann Klages, and Coen Hofstede, for conversations that provided helpful insights in the initial preparation stages of this manuscript, and Tobias Binder for helping with data collection in the 2018 EastGRIP season. We acknowledge the use of software from Open Polar Radar generated with support from the University of Kansas, NASA grants 80NSSC20K1242 and 80NSSC21K0753, and NSF grants OPP-2027615, OPP-2019719, OPP-1739003, IIS-1838230, RISE-2126503, RISE-2127606, and RISE-2126468. The authors would like to thank Aspen Technology, Inc. for providing software licenses and support. For the EGRIP-NOR-2018 and NEGIS-FLOW-2022 airborne radar campaigns, we acknowl-

edge support via the AWI funding grants AWI_PA_02097 and AWI_PA_02128.

EGRIP is directed and organized by the Centre for Ice and Climate at the Niels Bohr Institute, University of Copenhagen. It is supported by funding agencies and institutions in Denmark (A. P. Møller Foundation, University of Copenhagen), USA (US National Science Foundation, Office of Polar Programs), Germany (Alfred Wegener Institute, Helmholtz Centre for Polar and Marine Research), Japan (National Institute of Polar Research and Arctic Challenge for Sustainability), Norway (University of Bergen and Trond Mohn Foundation), Switzerland (Swiss National Science Foundation), France (French Polar Institute Paul-Emile Victor, Institute for Geosciences and Environmental research), Canada (University of Manitoba) and China (Chinese Academy of Sciences and Beijing Normal University).

CMC was funded by the Alfred Wegener Institute's INSPIRES III programme. SF was funded by the Walter Benjamin Programme of the Deutsche Forschungsgemeinschaft (DFG, German Research Foundation; project number 506043073).

Financial support. This research has been supported by the Alfred Wegener Institute Helmholtz Centre for Polar and Marine Research (INSPIRES III) and Deutsche Forschungsgemeinschaft (DFG, German Research Foundation; project number 506043073).

The article processing charges for this open-access publication were covered by the Alfred-Wegener-Institut Helmholtz-Zentrum für Polar- und Meeresforschung.

Review statement. This paper was edited by Stephen Livingstone and reviewed by Edouard Ravier and Kiya Riverman.

References

Al-Ibadi, M., Sprick, J., Athinarapu, S., Stumpf, T., Paden, J., Leuschen, C. J., Rodriguez, F., Xu, M., Crandall, D., Fox, G., Burgess, D., Sharp, M., Copland, L., and Van Wychen, W.: DEM extraction of the basal topography of the Canadian Archipelago Ice Caps via 2D automated layer-tracker, IGARSS, https://doi.org/10.1109/IGARSS.2017.8127114, 2017.

Alley, R. B., Holschuh, N., MacAyeal, D. R., Parizek, B. R., Zoet, L., Riverman, K., Muto, A., Christianson, K., Clyne, E., Anandakrishnan, S., Stevens, N., Smith, A., Arthern, R., Bingham, R., Brisbourne, A., Eisen, O., Hofstede, C., Kulessa, B., Sterns, L., Winberry, P., Bodart, J., Borthwick, L., Case, E., Gustafson, C., Kingslake, J., Ockenden, H., Schoonman, C., and Schwans, E.: Bedforms of Thwaites Glacier, West Antarctica: Character and Origin, Journal of Geophysical Research: Earth Surface, 126, https://doi.org/10.1029/2021JF006339, 2021.

Andersen, J. K., Rathmann, N., Hvidberg, C. S., Grinsted, A., Kusk, A., Merryman Boncori, J. P., and Mouginot, J.: Episodic Subglacial Drainage Cascades Below the Northeast Greenland Ice Stream, Geophysical Research Letters, 50, https://doi.org/10.1029/2023gl103240, 2023.

Anderson, J. B. and Fretwell, L. O.: Geomorphology of the onset area of a paleo-ice stream, Marguerite Bay, Antarctic Peninsula, Earth Surface Processes and Landforms, 33, 503–512, https://doi.org/10.1002/esp.1662, 2008.

Aschwanden, A., Fahnestock, M. A., and Truffer, M.: Complex Greenland outlet glacier flow captured, Nature Communications, 7, https://doi.org/10.1038/ncomms10524, 2016.

Bamber, J. L., Vaughan, D. G., and Joughin, I.: Widespread Complex Flow in the Interior of the Antarctic Ice Sheet, Science, 287, https://doi.org/10.1126/science.287.5456.1248, 2000.

Barchyn, T. E., Dowling, T. P. F., Stokes, C. R., and Hugenholtz, C. H.: Subglacial bed form morphology controlled by ice speed and sediment thickness, Geophysical Research Letters, 43, 7572–7580, https://doi.org/10.1002/2016gl069558, 2016.

Bingham, R. G., Vaughan, D. G., King, E. C., Davies, D., Cornford, S. L., Smith, A. M., Arthern, R. J., Brisbourne, A. M., De Rydt, J., Graham, A. G. C., Spagnolo, M., Marsh, O. J., and Shean, D. E.: Diverse landscapes beneath Pine Island Glacier influence ice flow, Nature Communications, 8, https://doi.org/10.1038/s41467-017-01597-y, 2017.

Bons, P. D., Jansen, D., Mundel, F., Bauer, C. C., Binder, T., Eisen, O., Jessell, M. W., Llorens, M. G., Steinbach, F., Steinhage, D., and Weikusat, I.: Converging flow and anisotropy cause large-scale folding in Greenland's ice sheet, Nature Communications, 7, https://doi.org/10.1038/ncomms11427, 2016.

Bons, P. D., de Riese, T., Franke, S., Llorens, M.-G., Sachau, T., Stoll, N., Weikusat, I., Westhoff, J., and Zhang, Y.: Comment on "Exceptionally high heat flux needed to sustain the Northeast Greenland Ice Stream" by Smith-Johnsen et al. (2020), The Cryosphere, 15, 2251–2254, https://doi.org/10.5194/tc-15-2251-2021, 2021.

Canals, M., Urgeles, R., and Calafat, A. M.: Deep sea-floor evidence of past ice streams off the Antarctic Peninsula., Geology, 28, 31–34, https://doi.org/10.1130/0091-7613(2000)028<0031:DSEOPI>2.0.CO;2, 2000.

Carter, C. M., Franke, S., Helm, V., Jansen, D., Paden, J. D., and Eisen, O.: High-resolution Digital Elevation Model of subglacial topography in the onset region of the Northeast Greenland Ice Stream, generated from swath radar imaging, PANGAEA [data set], https://doi.org/10.1594/PANGAEA.972422, 2025.

Chandler, B. M. P., Lovell, H., Boston, C. M., Lukas, S., Barr, I. D., Benediktsson, Í. Ö., Benn, D. I., Clark, C. D., Darvill, C. M., Evans, D. J. A., Ewertowski, M., Loibl, D., Margold, M., Otto, J.-C., Roberts, D. H., Stokes, C. R., Storrar, R. D., and Stroeven, A. P.: Glacial geomorphological mapping: a review of approaches and frameworks for best practice, Earth-Science Reviews, 806–846, https://doi.org/10.1016/j.earscirev.2018.07.015, 2018.

Christianson, K., Peters, L. E., Alley, R. B., Anandakrishnan, S., Jacobel, R. W., Riverman, K. L., Muto, A., and Keisling, B. A.: Dilatant till facilitates ice-stream flow in northeast Greenland, Earth and Planetary Science Letters, 401, 57–69, https://doi.org/10.1016/J.EPSL.2014.05.060, 2014.

Chu, W., Schroeder, D. M., Seroussi, H., Creyts, T. T., and Bell, R. E.: Complex Basal Thermal Transition Near the Onset of Petermann Glacier, Greenland, Journal of Geophysical Research: Earth Surface, 123, 985–995, https://doi.org/10.1029/2017jf004561, 2018.

Clark, C. D.: Mega-scale glacial lineations and cross-cutting ice-flow landforms, Earth Surface Processes and Landforms, 18, 1–29, https://doi.org/10.1002/esp.3290180102, 1993.

Clark, C. D., Tulaczyk, S. M., Stokes, C. R., and Canals, M.: A groove-ploughing theory for the production of mega-scale glacial lineations, and implications for ice-stream mechanics, Journal of Glaciology, 49, 240–256, https://doi.org/10.3189/172756503781830719, 2003.

De Angelis, H. and Kleman, J.: Palaeo-ice-stream onsets: examples from the north-eastern Laurentide Ice Sheet, Earth Surface Processes and Landforms, 33, 560–572, https://doi.org/10.1002/esp.1663, 2008.

Dowdeswell, E. K., Todd, B. J., and Dowdeswell, J. A.: Crag-and-tail features: convergent ice flow through Eclipse Sound, Baffin Island, Arctic Canada, in: Atlas of Submarine Glacial Landforms: Modern, Quaternary and Ancient, edited by: Dowdeswell, J. A., Canals, M., Jakobsson, M., Todd, B. J., Dowdeswell, E. K., and Hogan, K. A., Geological Society, London, https://doi.org/10.1144/M46, 2016.

Dowdeswell, J. A., Hogan, K. A., Evans, J., Noormets, R., Ó Cofaigh, C., and Ottesen, D.: Past ice-sheet flow east of Svalbard inferred from streamlined subglacial landforms, Geology, 38, 163–166, https://doi.org/10.1130/g30621.1, 2010.

Dowdeswell, J. A., Hogan, K. A., Ó Cofaigh, C., Fugelli, E. M. G., Evans, J., and Noormets, R.: Late Quaternary ice flow in a West Greenland fjord and cross-shelf trough system: submarine landforms from Rink Isbrae to Uummannaq shelf and slope, Quaternary Science Reviews, 92, 292–309, https://doi.org/10.1016/j.quascirev.2013.09.007, 2014.

Dubé-Loubert, H., Roy, M., Veillette, J. J., Brouard, E., Schaefer, J. M., and Wittmann, H.: The role of glacial dynamics in the development of ice divides and the Horseshoe Intersection Zone of the northeastern Labrador Sector of the Laurentide Ice Sheet, Geomorphology, 387, https://doi.org/10.1016/j.geomorph.2021.107777, 2021.

Ely, J. C., Clark, C. D., Spagnolo, M., Stokes, C. R., Greenwood, S. L., Hughes, A. L. C., Dunlop, P., and Hess, D.: Do subglacial bedforms comprise a size and shape continuum?, Geomorphology, 257, 108–119, https://doi.org/10.1016/j.geomorph.2016.01.001, 2016.

Ely, J. C., Stevens, D., Clark, C. D., and Butcher, F. E. G.: Numerical modelling of subglacial ribs, drumlins, herringbones, and mega-scale glacial lineations reveals their developmental trajectories and transitions, Earth Surface Processes and Landforms, https://doi.org/10.1002/esp.5529, 2022.

Eyles, N. and Doughty, M.: Glacially-streamlined hard and soft beds of the paleo- Ontario ice stream in Southern Ontario and New York state, Sedimentary Geology, 338, 51–71, https://doi.org/10.1016/j.sedgeo.2016.01.019, 2016.

Eyles, N., Putkinen, N., Sookhan, S., and Arbelaez-Moreno, L.: Erosional origin of drumlins and megaridges, Sedimentary Geology, 338, 2–23, https://doi.org/10.1016/j.sedgeo.2016.01.006, 2016.

Eyles, N., Arbelaez Moreno, L., and Sookhan, S.: Ice streams of the Late Wisconsin Cordilleran Ice Sheet in western North America, Quaternary Science Reviews, 179, 87–122, https://doi.org/10.1016/j.quascirev.2017.10.027, 2018.

Fahnestock, M., Abdalati, W., Joughin, I., Brozena, J., and Gogineni, P.: High geothermal heat flow, basal melt, and the origin of rapid ice flow in central Greenland, Science, 294, 2338–2342, https://doi.org/10.1126/science.1065370, 2001.

Fowler, A. C.: The formation of subglacial streams and mega-scale glacial lineations, Proceedings of the Royal Society A, 466, 3181–3201, https://doi.org/10.1098/rspa.2010.0009, 2010.

Franke, S., Jansen, D., Binder, T., Dörr, N., Helm, V., Paden, J., Steinhage, D., and Eisen, O.: Bed topography and subglacial landforms in the onset region of the Northeast Greenland Ice Stream, Annals of Glaciology, 61, 143–153, https://doi.org/10.1017/aog.2020.12, 2020.

Franke, S., Jansen, D., Beyer, S., Neckel, N., Binder, T., Paden, J., and Eisen, O.: Complex Basal Conditions and Their Influence on Ice Flow at the Onset of the Northeast Greenland Ice Stream, Journal of Geophysical Research: Earth Surface, 126, https://doi.org/10.1029/2020JF005689, 2021.

Franke, S., Bons, P. D., Westhoff, J., Weikusat, I., Binder, T., Streng, K., Steinhage, D., Helm, V., Eisen, O., Paden, J. D., Eagles, G., and Jansen, D.: Holocene ice-stream shutdown and drainage basin reconfiguration in northeast Greenland, Nature Geoscience, 1–7, https://doi.org/10.1038/s41561-022-01082-2, 2022a.

Franke, S., Jansen, D., Binder, T., Paden, J. D., Dörr, N., Gerber, T. A., Miller, H., Dahl-Jensen, D., Helm, V., Steinhage, D., Weikusat, I., Wilhelms, F., and Eisen, O.: Airborne ultra-wideband radar sounding over the shear margins and along flow lines at the onset region of the Northeast Greenland Ice Stream, Earth Syst. Sci. Data, 14, 763–779, https://doi.org/10.5194/essd-14-763-2022, 2022b.

Gardner, A., Fahnestock, M., and Scambos, T. A.: MEaSUREs ITS_LIVE Regional Glacier and Ice Sheet Surface Velocities (1), NASA National Snow and Ice Data Center Distributed Active Archive Center [data set], https://doi.org/10.5067/6II6VW8LLWJ7, 2022.

Gerber, T. A., Lilien, D. A., Rathmann, N. M., Franke, S., Young, T. J., Valero-Delgado, F., Ershadi, M. R., Drews, R., Zeising, O., Humbert, A., Stoll, N., Weikusat, I., Grinsted, A., Hvidberg, C. S., Jansen, D., Miller, H., Helm, V., Steinhage, D., O'Neill, C., Paden, J., Gogineni, S. P., Dahl-Jensen, D., and Eisen, O.: Crystal orientation fabric anisotropy causes directional hardening of the Northeast Greenland Ice Stream, Nat. Commun., 14, 2653, https://doi.org/10.1038/s41467-023-38139-8, 2023.

Graham, A. G. C., Larter, R. D., Gohl, K., Hillenbrand, C. D., Smith, J. A., and Kuhn, G.: Bedform signature of a West Antarctic palaeo-ice stream reveals a multi-temporal record of flow and substrate control, Quaternary Science Reviews, 28, 2774–2793, https://doi.org/10.1016/J.QUASCIREV.2009.07.003, 2009.

Gudmundsson, G. H. and Jenkins, A.: Ice-flow velocities on Rutford Ice Stream, West Antarctica, are stable over decadal timescales, Journal of Glaciology, 55, 339–344, https://doi.org/10.3189/002214309788608697, 2017.

Hale, R. D., Miller, H., Gogineni, S., Yan, J. B., Rodriguez-Morales, F., Leuschen, C. J., Paden, J. D., Li, J., Binder, T., Steinhage, D., Gehrmann, M., and Braaten, D.: Multi-Channel Ultra-Wideband Radar Sounder and Imager, IGARSS, 2112–2115, https://doi.org/10.1109/IGARSS.2016.7729545, 2016.

Hodder, T. J., Ross, M., and Menzies, J.: Sedimentary record of ice divide migration and ice streams in the Keewatin core region of the Laurentide Ice Sheet, Sedimentary Geology, 338, 97–114, https://doi.org/10.1016/j.sedgeo.2016.01.001, 2016.

Hoffman, A. O., Holschuh, N., Mueller, M., Paden, J., Muto, A., Ariho, G., Brigham, C., Christian, J. E., Davidge, L., Heitmann,

E., Hills, B., Horlings, A., Morey, S., O'Connor, G., Fudge, T. J., Steig, E. J., and Christianson, K.: Scars of tectonism promote ice-sheet nucleation from Hercules Dome into West Antarctica, Nature Geoscience, 1005–1013, https://doi.org/10.1038/s41561-023-01265-5, 2023.

Holschuh, N., Lilien, D. A., and Christianson, K.: Thermal Weakening, Convergent Flow, and Vertical Heat Transport in the Northeast Greenland Ice Stream Shear Margins, Geophysical Research Letters, 46, 8184–8193, https://doi.org/10.1029/2019GL083436, 2019.

Holschuh, N., Christianson, K., Paden, J., Alley, R. B., and Anandakrishnan, S.: Linking postglacial landscapes to glacier dynamics using swath radar at Thwaites glacier, Antarctica, Geology, 48, 268–272, https://doi.org/10.1130/G46772.1, 2020.

Hvidberg, C. S., Grinsted, A., Dahl-Jensen, D., Khan, S. A., Kusk, A., Andersen, J. K., Neckel, N., Solgaard, A., Karlsson, N. B., Kjær, H. A., and Vallelonga, P.: Surface velocity of the Northeast Greenland Ice Stream (NEGIS): assessment of interior velocities derived from satellite data by GPS, The Cryosphere, 14, 3487–3502, https://doi.org/10.5194/tc-14-3487-2020, 2020.

Jamieson, S. S. R., Stokes, C. R., Livingstone, S. J., Vieli, A., Ó Cofaigh, C., Hillenbrand, C.-D., and Spagnolo, M.: Subglacial processes on an Antarctic ice stream bed. 2: Can modelled ice dynamics explain the morphology of mega-scale glacial lineations?, Journal of Glaciology, 62, 285–298, https://doi.org/10.1017/jog.2016.19, 2016.

Jansen, D., Franke, S., Bauer, C. C., Binder, T., Dahl-Jensen, D., Eichler, J., Eisen, O., Hu, Y., Kerch, J., Llorens, M. G., Miller, H., Neckel, N., Paden, J., de Riese, T., Sachau, T., Stoll, N., Weikusat, I., Wilhelms, F., Zhang, Y., and Bons, P. D.: Shear margins in upper half of Northeast Greenland Ice Stream were established two millennia ago, Nat. Commun., 15, 1193, https://doi.org/10.1038/s41467-024-45021-8, 2024.

Jezek, K., Wu, X., Gogineni, P., Rodríguez, E., Freeman, A., Rodriguez-Morales, F., and Clark, C. D.: Radar images of the bed of the Greenland Ice Sheet, Geophysical Research Letters, 38, https://doi.org/10.1029/2010gl045519, 2011.

Joughin, I., Smith, B. E., and Howat, I. M.: A complete map of Greenland ice velocity derived from satellite data collected over 20 years, Journal of Glaciology, 64, 1–11, https://doi.org/10.1017/JOG.2017.73, 2018.

Kehew, A. E., Piotrowski, J. A., and Jørgensen, F.: Tunnel valleys: Concepts and controversies – A review, Earth-Science Reviews, 113, 33–58, https://doi.org/10.1016/j.earscirev.2012.02.002, 2012.

King, E. C., Woodward, J., and Smith, A. M.: Seismic and radar observations of subglacial bed forms beneath the onset zone of Rutford Ice Stream, Antarctica, Journal of Glaciology, 53, 665–672, https://doi.org/10.3189/002214307784409216, 2007.

King, E. C., Hindmarsh, R. C. A., and Stokes, C. R.: Formation of mega-scale glacial lineations observed beneath a West Antarctic ice stream, Nature Geoscience, 2, 585–588, https://doi.org/10.1038/ngeo581, 2009.

King, E. C., Pritchard, H. D., and Smith, A. M.: Subglacial landforms beneath Rutford Ice Stream, Antarctica: detailed bed topography from ice-penetrating radar, Earth Syst. Sci. Data, 8, 151–158, https://doi.org/10.5194/essd-8-151-2016, 2016.

Krieger, L., Floricioiu, D., and Neckel, N.: Drainage basin delineation for outlet glaciers of Northeast Greenland based on Sentinel-1 ice velocities and TanDEM-X elevations, Remote Sensing of Environment, 237, https://doi.org/10.1016/j.rse.2019.111483, 2019.

Law, R., Christoffersen, P., MacKie, E., Cook, S., Haseloff, M., and Gagliardini, O.: Complex motion of Greenland Ice Sheet outlet glaciers with basal temperate ice, Science Advances, 9, eabq5180, https://doi.org/10.1126/sciadv.abq5180, 2023.

Livingstone, S. J. and Clark, C. D.: Morphological properties of tunnel valleys of the southern sector of the Laurentide Ice Sheet and implications for their formation, Earth Surf. Dynam., 4, 567–589, https://doi.org/10.5194/esurf-4-567-2016, 2016.

Margold, M., Stokes, C. R., and Clark, C. D.: Ice streams in the Laurentide Ice Sheet: Identification, characteristics and comparison to modern ice sheets, Earth-Science Reviews, 143, 117–146, https://doi.org/10.1016/j.earscirev.2015.01.011, 2015a.

Margold, M., Stokes, C. R., Clark, C. D., and Kleman, J.: Ice streams in the Laurentide Ice Sheet: a new mapping inventory, Journal of Maps, 11, 380–395, https://doi.org/10.1080/17445647.2014.912036, 2015b.

Margold, M., Stokes, C. R., and Clark, C. D.: Reconciling records of ice streaming and ice margin retreat to produce a palaeogeographic reconstruction of the deglaciation of the Laurentide Ice Sheet, Quartenary Science Reviews, 189, 1–30, https://doi.org/10.1016/j.quascirev.2018.03.013, 2018.

Morlighem, M., Williams, C. N., Rignot, E., An, L., Arndt, J. E., Bamber, J. L., Catania, G., Chauche, N., Dowdeswell, J. A., Dorschel, B., Fenty, I., Hogan, K., Howat, I., Hubbard, A., Jakobsson, M., Jordan, T. M., Kjeldsen, K. K., Millan, R., Mayer, L., Mouginot, J., Noel, B. P. Y., O'Cofaigh, C., Palmer, S., Rysgaard, S., Seroussi, H., Siegert, M. J., Slabon, P., Straneo, F., van den Broeke, M. R., Weinrebe, W., Wood, M., and Zinglersen, K. B.: BedMachine v3: Complete Bed Topography and Ocean Bathymetry Mapping of Greenland From Multibeam Echo Sounding Combined With Mass Conservation, Geophys. Res. Lett., 44, 11051–11061, https://doi.org/10.1002/2017GL074954, 2017.

Morlighem, M., Williams, C., Rignot, E., An, L., Arndt, J. E., Bamber, J. L., Catania, G., Chauche, N., Dowdeswell, J. A., Dorschel, B., Fenty, I., Hogan, K., Howat, I., Hubbard, A. L., Jakobsson, M., Jordan, T. M., Kjeldsen, K. K., Millan, R., Mayer, L., Mouginot, J., Noel, B. P. Y., O'Cofaigh, C., Palmer, S. J., Rysgaard, S., Seroussi, H., Siegert, M. J., Slabon, P., Straneo, F., van den Broeke, M. R., Weinrebe, W., Wood, M., and Zinglersen, K. B.: IceBridge BedMachine Greenland, Version 5, NASA National Snow and Ice Data Center Distributed Active Archive Center [data set], https://doi.org/10.5067/GMEVBWFLWA7X, 2022.

Mouginot, J., Rignot, E., Bjork, A. A., van den Broeke, M., Millan, R., Morlighem, M., Noel, B., Scheuchl, B., and Wood, M.: Forty-six years of Greenland Ice Sheet mass balance from 1972 to 2018, Proc. Natl. Acad. Sci. USA, 116, 9239–9244, https://doi.org/10.1073/pnas.1904242116, 2019.

Mulligan, R. P. M., Eyles, C. H., and Marich, A. S.: Subglacial and ice-marginal landforms in south-central Ontario: implications for ice-sheet reconfiguration during deglaciation, Boreas, 48, 635–657, https://doi.org/10.1111/bor.12372, 2019.

Newton, M., Evans, D. J. A., Roberts, D. H., and Stokes, C. R.: Bedrock mega-grooves in glaciated terrain: A review, Earth-Science Reviews, 185, 57–79, https://doi.org/10.1016/j.earscirev.2018.03.007, 2018.

Newton, M., Stokes, C. R., Roberts, D. H., and Evans, D. J. A.: Characteristics and formation of bedrock mega-grooves (BMGs) in glaciated terrain: 1 – morphometric analyses, Geomorphology, 427, https://doi.org/10.1016/j.geomorph.2023.108619, 2023.

Nitsche, F. O., Larter, R. D., Gohl, K., Graham, A. G. C., and Kuhn, G.: Crag-and-tail features on the Amundsen Sea continental shelf, West Antarctica, in: Atlas of Submarine Glacial Landforms: Modern, Quaternary and Ancient, edited by: Dowdeswell, J. A., Canals, M., Jakobsson, M., Todd, B. J., Dowdeswell, E. K., and Hogan, K., Geological Society, London, https://doi.org/10.1144/M46, 2016.

Open Polar Radar: opr (Version 3.0.1), GitLab [computer software], https://gitlab.com/openpolarradar/opr/ (last access: 23 October 2025), 2023.

Otosaka, I. N., Shepherd, A., Ivins, E. R., Schlegel, N.-J., Amory, C., van den Broeke, M. R., Horwath, M., Joughin, I., King, M. D., Krinner, G., Nowicki, S., Payne, A. J., Rignot, E., Scambos, T., Simon, K. M., Smith, B. E., Sørensen, L. S., Velicogna, I., Whitehouse, P. L., A, G., Agosta, C., Ahlstrøm, A. P., Blazquez, A., Colgan, W., Engdahl, M. E., Fettweis, X., Forsberg, R., Gallée, H., Gardner, A., Gilbert, L., Gourmelen, N., Groh, A., Gunter, B. C., Harig, C., Helm, V., Khan, S. A., Kittel, C., Konrad, H., Langen, P. L., Lecavalier, B. S., Liang, C.-C., Loomis, B. D., McMillan, M., Melini, D., Mernild, S. H., Mottram, R., Mouginot, J., Nilsson, J., Noël, B., Pattle, M. E., Peltier, W. R., Pie, N., Roca, M., Sasgen, I., Save, H. V., Seo, K.-W., Scheuchl, B., Schrama, E. J. O., Schröder, L., Simonsen, S. B., Slater, T., Spada, G., Sutterley, T. C., Vishwakarma, B. D., van Wessem, J. M., Wiese, D., van der Wal, W., and Wouters, B.: Mass balance of the Greenland and Antarctic ice sheets from 1992 to 2020, Earth Syst. Sci. Data, 15, 1597–1616, https://doi.org/10.5194/essd-15-1597-2023, 2023.

Paden, J., Akins, T., Dunson, D., Allen, C., and Gogineni, P.: Ice-sheet bed 3-D tomography, Journal of Glaciology, 56, 3–11, https://doi.org/10.3189/002214310791190811, 2010.

QGIS: QGIS Geographic Information System, Open Source Geospatial Foundation Project, http://qgis.org (last access: 20 October 2025), 2025.

Rathmann, N. M. and Lilien, D. A.: Inferred basal friction and mass flux affected by crystal-orientation fabrics, Journal of Glaciology, 68, 236–252, https://doi.org/10.1017/JOG.2021.88, 2022.

Rice, J. M., Ross, M., Paulen, R. C., Kelley, S. E., and Briner, J. P.: A GIS-based multi-proxy analysis of the evolution of subglacial dynamics of the Quebec–Labrador ice dome, northeastern Quebec, Canada, Earth Surface Processes and Landforms, 45, 3155–3177, https://doi.org/10.1002/esp.4957, 2020.

Rice, J. M., Ross, M., Campbell, H. E., Paulen, R. C., and Mcclenaghan, M. B.: Net evolution of subglacial sediment transport in the Quebec–Labrador sector of the Laurentide Ice Sheet, Canadian Journal of Earth Sciences, 61, 524–542, https://doi.org/10.1139/cjes-2023-0050, 2024.

Riverman, K. L., Anandakrishnan, S., Alley, R. B., Holschuh, N., Dow, C. F., Muto, A., Parizek, B. R., Christianson, K., and Peters, L. E.: Wet subglacial bedforms of the NE Greenland Ice Stream shear margins, Annals of Glaciology, 60, 91–99, https://doi.org/10.1017/aog.2019.43, 2019.

Roberts, D. H., Grimoldi, E., Callard, L., Evans, D. J. A., Clark, C. D., Stewart, H. A., Dove, D., Saher, M., Ó Cofaigh, C., Chiverrell, R. C., Bateman, M. D., Moreton, S. G., Bradwell, T., Fabel, D., and Medialdea, A.: The mixed-bed glacial landform imprint of the North Sea Lobe in the western North Sea, Earth Surface Processes and Landforms, 44, 1233–1258, https://doi.org/10.1002/esp.4569, 2019.

Rysgaard, S., Bendtsen, J., Mortensen, J., and Sejr, M. K.: High geothermal heat flux in close proximity to the Northeast Greenland Ice Stream, Scientific Reports, 8, https://doi.org/10.1038/s41598-018-19244-x, 2018.

Schlegel, R., Murray, T., Smith, A. M., Brisbourne, A. M., Booth, A. D., King, E. C., and Clark, R. A.: Radar Derived Subglacial Properties and Landforms Beneath Rutford Ice Stream, West Antarctica, Journal of Geophysical Research: Earth Surface, 127, https://doi.org/10.1029/2021jf006349, 2022.

Shaw, J., Pugin, A., and Young, R. R.: A meltwater origin for Antarctic shelf bedforms with special attention to megalineations, Geomorphology, 102, 364–375, https://doi.org/10.1016/j.geomorph.2008.04.005, 2008.

Shepherd, A., Ivins, E., Rignot, E., Smith, B., van den Broeke, M., Velicogna, I., Whitehouse, P., Briggs, K., Joughin, I., Krinner, G., Nowicki, S., Payne, T., Scambos, T., Schlegel, N., A, G., Agosta, C., Ahlstrøm, A., Babonis, G., Barletta, V. R., Bjørk, A. A., Blazquez, A., Bonin, J., Colgan, W., Csatho, B., Cullather, R., Engdahl, M. E., Felikson, D., Fettweis, X., Forsberg, R., Hogg, A. E., Gallee, H., Gardner, A., Gilbert, L., Gourmelen, N., Groh, A., Gunter, B., Hanna, E., Harig, C., Helm, V., Horvath, A., Horwath, M., Khan, S., Kjeldsen, K. K., Konrad, H., Langen, P. L., Lecavalier, B., Loomis, B., Luthcke, S., McMillan, M., Melini, D., Mernild, S., Mohajerani, Y., Moore, P., Mottram, R., Mouginot, J., Moyano, G., Muir, A., Nagler, T., Nield, G., Nilsson, J., Noël, B., Otosaka, I., Pattle, M. E., Peltier, W. R., Pie, N., Rietbroek, R., Rott, H., Sandberg Sørensen, L., Sasgen, I., Save, H., Scheuchl, B., Schrama, E., Schröder, L., Seo, K.-W., Simonsen, S. B., Slater, T., Spada, G., Sutterley, T., Talpe, M., Tarasov, L., van de Berg, W. J., van der Wal, W., van Wessem, M., Vishwakarma, B. D., Wiese, D., Wilton, D., Wagner, T., Wouters, B., Wuite, J., and The, I. T.: Mass balance of the Greenland Ice Sheet from 1992 to 2018, Nature, 579, 233–239, https://doi.org/10.1038/s41586-019-1855-2, 2020.

Smith-Johnsen, S., de Fleurian, B., Schlegel, N., Seroussi, H., and Nisancioglu, K.: Exceptionally high heat flux needed to sustain the Northeast Greenland Ice Stream, The Cryosphere, 14, 841–854, https://doi.org/10.5194/tc-14-841-2020, 2020.

Spagnolo, M., Clark, C. D., Ely, J. C., Stokes, C. R., Anderson, J. B., Andreassen, K., Graham, A. G. C., and King, E. C.: Size, shape and spatial arrangement of mega-scale glacial lineations from a large and diverse dataset, Earth Surface Processes and Landforms, 39, 1432–1448, https://doi.org/10.1002/esp.3532, 2014.

Stokes, C. R. and Clark, C. D.: Ice stream shear margin moraines, Earth Surface Processes and Landforms, 27, 547–558, https://doi.org/10.1002/ESP.326, 2002a.

Stokes, C. R. and Clark, C. D.: Are long subglacial bedforms indicative of fast ice flow?, Boreas, 31, 239–249, https://doi.org/10.1111/J.1502-3885.2002.TB01070.X, 2002b.

Stokes, C. R., Margold, M., Clark, C. D., and Tarasov, L.: Ice stream activity scaled to ice sheet volume during Laurentide Ice Sheet deglaciation, Nature, 530, 322–326, https://doi.org/10.1038/nature16947, 2016.

Stokes, C. R., Spagnolo, M., Clark, C. D., Ó Cofaigh, C., Lian, O. B., and Dunstone, R. B.: Formation of mega-

scale glacial lineations on the Dubawnt Lake Ice Stream bed: 1. size, shape and spacing from a large remote sensing dataset, Quaternary Science Reviews, 77, 190–209, https://doi.org/10.1016/J.QUASCIREV.2013.06.003, 2013.

Stokes, C. R., Tarasov, L., Blomdin, R., Cronin, T. M., Fisher, T. G., Gyllencreutz, R., Hättestrand, C., Heyman, J., Hindmarsh, R. C. A., Hughes, A. L. C., Jakobsson, M., Kirchner, N., Livingstone, S. J., Margold, M., Murton, J. B., Noormets, R., Peltier, W. R., Peteet, D. M., Piper, D. J. W., Preusser, F., Renssen, H., Roberts, D. H., Roche, D. M., Saint-Ange, F., Stroeven, A. P., and Teller, J. T.: On the reconstruction of palaeo-ice sheets: Recent advances and future challenges, Quaternary Science Reviews, 125, 15–49, https://doi.org/10.1016/j.quascirev.2015.07.016, 2015.

Stoll, N., Weikusat, I., Jansen, D., Bons, P., Darányi, K., Westhoff, J., Llorens, M.-G., Wallis, D., Eichler, J., Saruya, T., Homma, T., Rasmussen, S. O., Sinnl, G., Svensson, A., Drury, M., Wilhelms, F., Kipfstuhl, S., Dahl-Jensen, D., and Kerch, J.: Linking crystallographic orientation and ice stream dynamics: evidence from the EastGRIP ice core, The Cryosphere, 19, 3805–3830, https://doi.org/10.5194/tc-19-3805-2025, 2025.

Tabone, I., Robinson, A., Montoya, M., and Alvarez-Solas, J.: Holocene thinning in central Greenland controlled by the Northeast Greenland Ice Stream, Nat. Commun., 15, 6434, https://doi.org/10.1038/s41467-024-50772-5, 2024.

Vérité, J., Ravier, É., Bourgeois, O., Pochat, S., Lelandais, T., Mourgues, R., Clark, C. D., Bessin, P., Peigné, D., and Atkinson, N.: Formation of ribbed bedforms below shear margins and lobes of palaeo-ice streams, The Cryosphere, 15, 2889–2916, https://doi.org/10.5194/tc-15-2889-2021, 2021.

Vérité, J., Ravier, É., Bourgeois, O., Bessin, P., and Pochat, S.: New metrics reveal the evolutionary continuum behind the morphological diversity of subglacial bedforms, Geomorphology, 427, https://doi.org/10.1016/j.geomorph.2023.108627, 2023.

Vérité, J., Ravier, É., Bourgeois, O., Pochat, S., and Bessin, P.: The kinematic significance of subglacial bedforms and their use in palaeo-glaciological reconstructions, Earth and Planetary Science Letters, 626, https://doi.org/10.1016/j.epsl.2023.118510, 2024.

Woodward, J. and King, E. C.: Radar surveys of the Rutford Ice Stream onset zone, West Antarctica: indications of flow (in)stability?, Annals of Glaciology, 50, 57–62, https://doi.org/10.3189/172756409789097469, 2009.

Zeising, O. and Humbert, A.: Indication of high basal melting at the EastGRIP drill site on the Northeast Greenland Ice Stream, The Cryosphere, 15, 3119–3128, https://doi.org/10.5194/tc-15-3119-2021, 2021.

Zoet, L. K., Rawling, J. E., Woodard, J. B., Barrette, N., and Mickelson, D. M.: Factors that contribute to the elongation of drumlins beneath the Green Bay Lobe, Laurentide Ice Sheet, Earth Surface Processes and Landforms, 46, 2540–2550, https://doi.org/10.1002/esp.5192, 2021.